

Supporting Information

***Cryogenic Luminescent Thermometers Based on
Multinuclear $\text{Eu}^{3+}/\text{Tb}^{3+}$ Mixed Lanthanide
Polyoxometalates***

Anna M. Kaczmarek*^a Jing Liu,^a Brecht Laforce,^b Laszlo Vincze,^b Kristof Van Hecke,^c and Rik Van Deun*^a

^a L³ - Luminescent Lanthanide Lab, Department of Inorganic and Physical Chemistry, Ghent University, Krijgslaan 281-S3, B-9000 Ghent, Belgium E

^b XMI group, Department of Analytical Chemistry, Ghent University, Krijgslaan 281-S3, B-9000 Ghent, Belgium

^c XStruct, Department of Inorganic and Physical Chemistry, Ghent University, Krijgslaan 281-S3, B-9000 Ghent, Belgium

E-mail: anna.kaczmarek@ugent.be, rik.vandeun@ugent.be

Experimental Section

Synthesis

All chemicals (analytical-grade) were purchased from Sigma-Aldrich or VWR and used without further purification. The compounds were prepared according to a modified synthesis based on that previously reported in literature.¹

0.4 mmol $(\text{NH}_4)_6\text{Mo}_7\text{O}_{24}\cdot 4\text{H}_2\text{O}$ was dissolved in 6 mL of distilled H_2O and 1 mL methanol at 50 °C. Next, $\text{Tb}(\text{NO}_3)_3\cdot x\text{H}_2\text{O}$, $\text{Tb}_{0.90}\text{Eu}_{0.10}(\text{NO}_3)_3\cdot x\text{H}_2\text{O}$ or $\text{Tb}_{0.95}\text{Eu}_{0.05}(\text{NO}_3)_3\cdot x\text{H}_2\text{O}$ (last two compounds are mixtures of two salts; $x = 5-6$) dissolved in 2 mL distilled water was added and left to stir at room temperature for 30 minutes. The solutions were filtered and the filtrate set up for crystallization through vapor diffusion of methanol into the water-methanol solution of the lanthanide polyoxometalates (at 7 °C). Crystals suitable for data collection were obtained after 1-3 days. They were filtered off and dried in air for luminescence measurements. A big strength of these materials is their easy preparation (both synthesis and crystallization process).

Characterization

For the reported structures X-ray intensity data were collected on an

Agilent Supernova Dual Source diffractometer equipped with an Atlas CCD detector using ω scans and MoK α ($\lambda = 0.71073 \text{ \AA}$) radiation for samples **P1** and **P2**. The images were interpreted and integrated with the program CrysAlisPro (Agilent Technologies).² Using Olex2,³ the structures were solved by direct methods using the ShelXS structure solution program and refined by full-matrix least-squares on F^2 using the ShelXL program package.⁴⁻⁵ All atoms were anisotropically refined. Hydrogen atoms could not be unequivocally located on solvent water or ammonium molecules, and were not included in the refinement. The crystals were measured at 100 K. ICSD reference numbers: ICSD 432526 (**P1**) and ICSD 432525 (**P2**).

Energy dispersive X-ray fluorescence (XRF) measurements were performed at the Ghent University Analytical Chemistry department, using an in-house developed μ XRF instrument.⁶ This instrument is equipped with a monochromatic microfocus source (XOS, USA) and an SDD detector (e2v, UK). The dried LnPOM crystals were placed between two 6 μm thin films of Mylar foil (SPEX SamplePrep, USA) on a polymer sample holder. XRF mappings of 10 by 10 points (step size 100 μm) with a live time of 10 s per point were performed, thus the retrieved spectra cover a relatively large area of the powder. The XRF spectra were

analyzed using the AXIL software package.⁷ The individual spectra were then summed to improve on the statistics. Monte-Carlo simulation aided quantification was used to calculate the relative presence of the lanthanide elements (Eu, Tb) present in the samples.⁸ In the procedure, a detailed simulation of the instrument is set up using measurements on reference materials to validate the parameters. Next, the sample is incorporated in the simulation and its composition is optimized until the simulated and experimental spectra coincide.

The luminescence of solid samples was studied. Solid powdered samples were put between quartz plates (Starna cuvettes for powdered samples, type 20/C/Q/0.2).

Luminescence measurements were performed on an Edinburgh Instruments FLSP920 UV-vis-NIR spectrometer setup. A 450W xenon lamp was used as the steady state excitation source. A Hamamatsu R928P photomultiplier tube was used to detect the emission signals in the near UV to visible range. The temperature dependent measurements were measured using an ARS closed cycle cryostat at a temperature range between 10 K – 310 K (with a temperature step ranging from 5 - 50 K).

In order to compare the measurements the same amounts of powders

were used as well as the same settings for each measurement (same slit size, step, and dwell time). All of the excitation spectra are recorded observing at the strongest f-f emission peak. All emission spectra in the manuscript have been corrected for detector response.

Table S1. Data collection and refinement statistic.

	P1	P2
Molecular formula	Tb _{11.81} Eu _{0.19} Mo ₈₇ O ₄₇₂	Tb _{3.68} Eu _{0.32} Mo ₂₉ O ₁₆₃
Formula weight (gmol⁻¹)	17804.60	6023.75
T (K)	100	100
λ (Å)	0.71073	0.71073
Crystal system	triclinic	triclinic
Space group	<i>P</i> -1	<i>P</i> -1
a (Å)	18.62032(13)	17.1832(2)
b (Å)	29.59902(16)	19.3527(3)
c (Å)	36.28676(17)	23.8426(2)
α (°)	86.5448(4)	85.827(1)
β (°)	88.2388(5)	87.525(1)
γ (°)	86.4840(5)	65.543(1)
V (Å³)	19917.9(2)	7197.35(16)
Z	2	2
ρ_{calc} (gcm⁻³)	2.969	2.780
2θ_{max} (°)	59.392	59.392
F(000)	16419.2	5562.7
Measured reflections	447068	158877
Unique reflections	101627	36369
Observed reflections (<i>I</i> > 2σ(<i>I</i>))	83777	26163
Parameters refined	5105	1753
R₁	0.0591	0.0668
wR₂	0.1329	0.1610
R₁ (all data)	0.0741	0.0998
wR₂ (all data)	0.1412	0.1858
Goodness-of-fit (GOF)	1.062	1.029
μ (mm⁻¹)	4.868	4.481
CCDC-entry	ICSD 432526	ICSD 432525

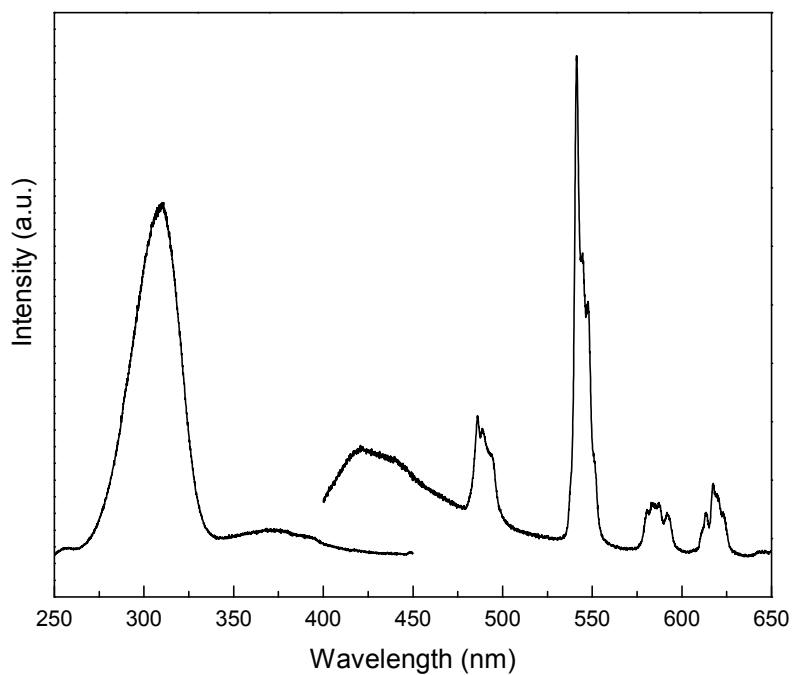


Figure S1 RT combined excitation-emission spectrum of TbPOM (excited at 310.0, emission observed at 544.0 nm).

Table S2 Assignment of f-f peaks in the emission spectrum of **TbPOM** (Figure S1).

Wavelength (nm)	Wavenumber (cm ⁻¹)	Transition
485.4	20602	⁵ D ₄ → ⁷ F ₆
540.2	18512	⁵ D ₄ → ⁷ F ₅
586.6	17047	⁵ D ₄ → ⁷ F ₄
618.2	16176	⁵ D ₄ → ⁷ F ₃

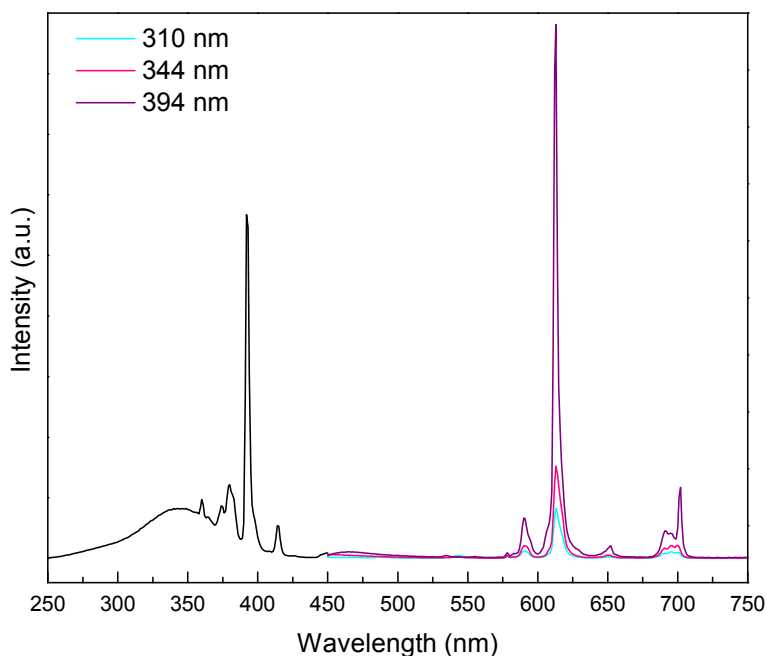


Figure S2 RT combined emission-excitation spectrum of **P2**. The compound has been excited at three different wavelengths: 310.0 nm, 344.0 nm, and 394.0 nm. In all cases the emission was observed at 612.6 nm.

Table S3 Assignment of f-f peaks in the excitation and emission spectra of **P2** (Figure S2).

Wavelength (nm)	Wavenumber (cm ⁻¹)	Transition
Excitation		
360.1	27770	⁵ D ₄ ← ⁷ F ₀
379.4	26357	⁵ G ₂ ← ⁷ F ₀
391.9	25517	⁵ L ₆ ← ⁷ F ₀
414.7	24114	⁵ D ₃ ← ⁷ F ₀
Emission		
579.1	17268	^b D ₀ → ⁷ F ₀
590.7	16929	^b D ₀ → ⁷ F ₁
612.6	16324	^b D ₀ → ⁷ F ₂
651.7	15344	^b D ₀ → ⁷ F ₃
701.8	14249	^b D ₀ → ⁷ F ₄

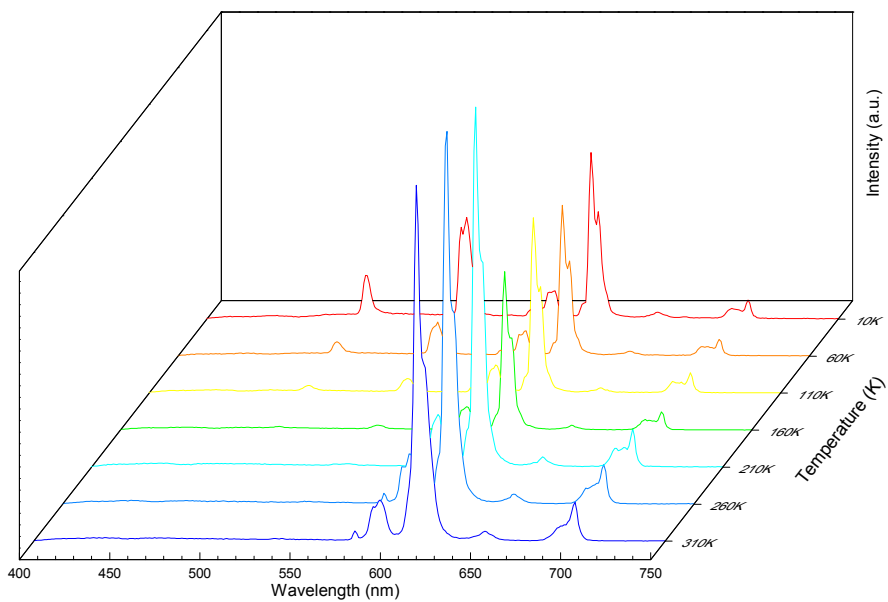


Figure S3 Emission map of **P1** measured in the 10 – 310 K temperature range (measurement step of 50 K). The intensity of the Eu^{3+} peaks significantly increases at 210 K. The sample was excited at 344.0 nm.

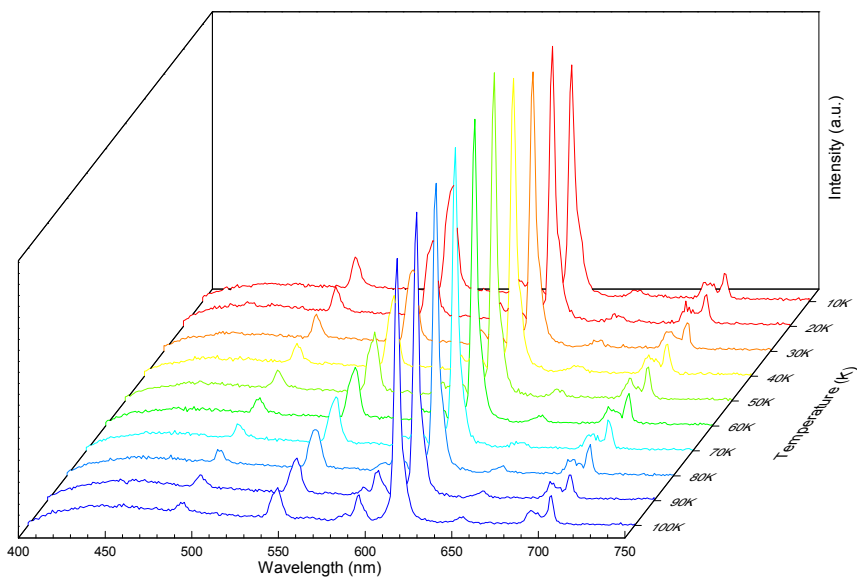


Figure S4 Emission map of **P2** in the 10 – 100 K temperature range (measurement step of 10 K). The sample was excited at 344.0 nm.

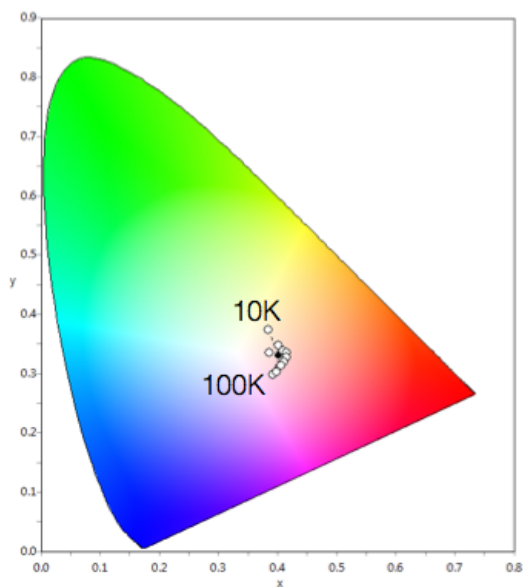


Figure S5 CIE diagram showing the **P2** sample color change with temperature change (10 – 100 K).

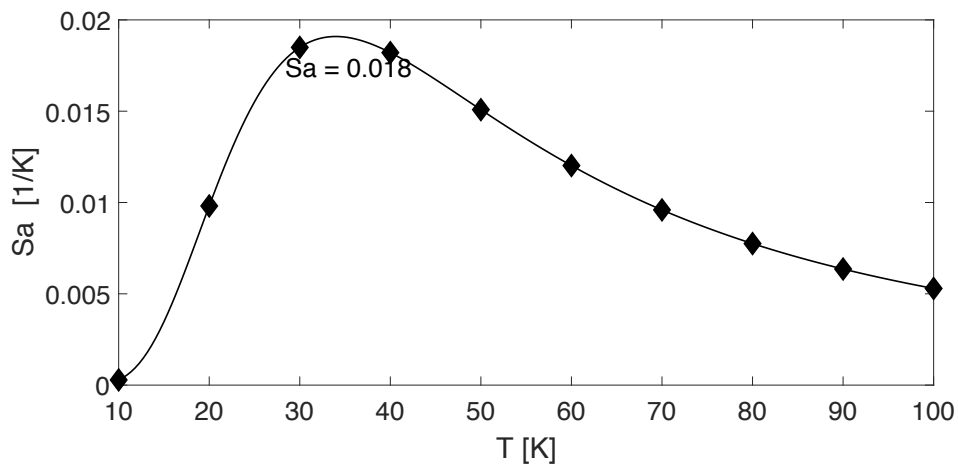


Figure S6 Plot showing the absolute sensitivity S_a values at different temperatures (10 – 100 K) for **P1**. The solid line is a guide for eyes.

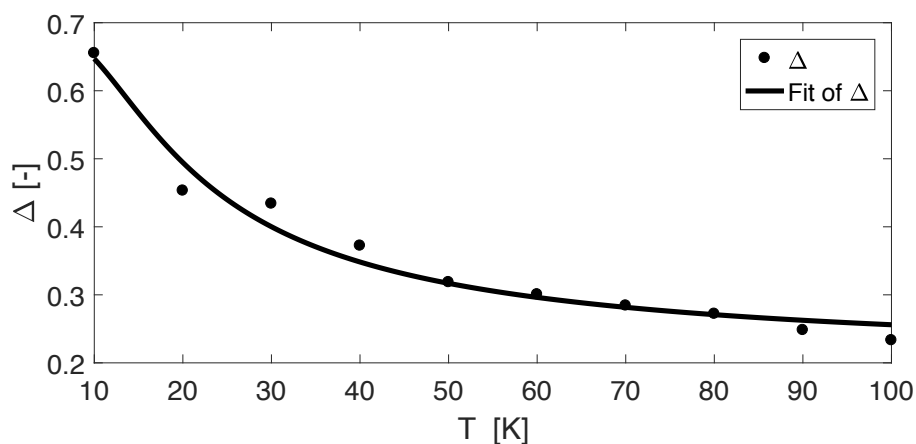


Figure S7 Plot presenting the calibration curve for **P2**. The open points depict the experimental Δ parameter and the solid line is the best fit of the experimental points using equation 2.

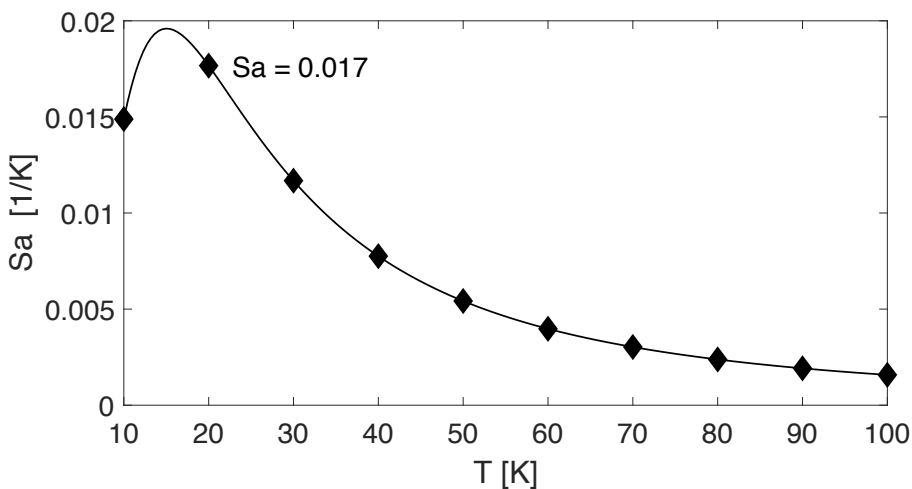


Figure S8 Plot showing the absolute sensitivity S_a values at different temperatures (10 – 100 K) for **P2**. The solid line is a guide for eyes.

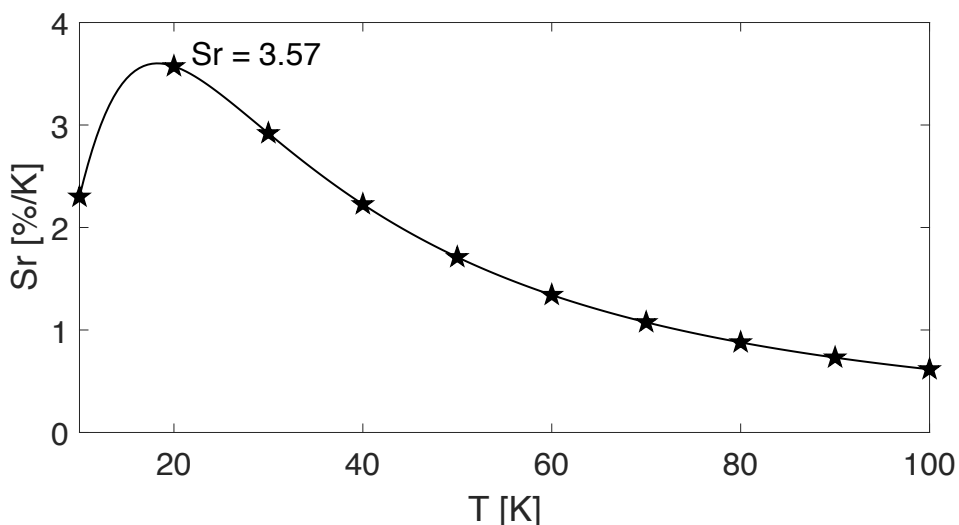


Figure S9 Plot showing the relative sensitivity S_r values at different temperatures (10 – 100 K) for **P2**. The solid line is a guide for eyes.

We have also made attempts to fit the **P2** compound with equation S1, which would assume the presence of a second non-radiative process, with an activation energy ΔE_2 (see Figure S10 below). Although equation S1 gave a better fit ($R^2 = 0.992$) than equation 2 ($R^2 = 0.971$) we doubt that there would be a difference in the number of non-radiative channels in **P1** and **P2** materials (which are very similar to each other). Therefore,

despite the slightly worse R^2 we have chosen to present the results calculated using equation 2 as we believe these are more correct.

$$\Delta = \frac{\Delta_0}{1 + \alpha_1 \exp\left(-\frac{\Delta E_1}{kBT}\right) + \alpha_2 \exp\left(-\frac{\Delta E_2}{kBT}\right)} \quad (S1)$$

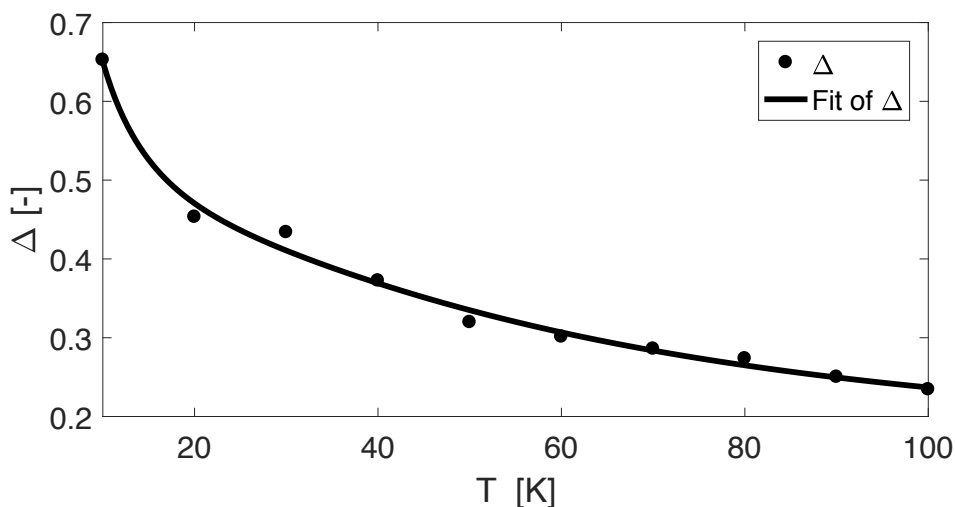


Figure S10 Plot presenting the calibration curve for **P2**. The open points depict the experimental Δ parameter and the solid line is the best fit of the experimental points using equation S1.

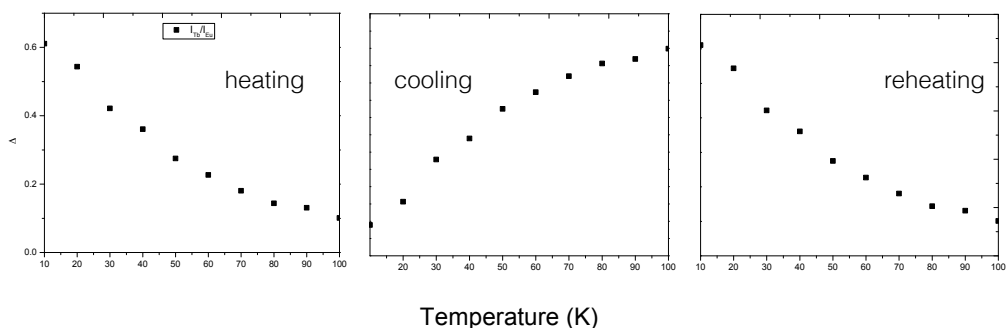


Figure S11 Plots showing heating, cooling and reheating tests of the **P1** material to show its stability. The Δ parameter remains stable throughout these tests.

Table S4 Overview of the relative sensitivity S_r (highest value) for recently reported ratiometric thermometer materials (only materials which were tested in the cryogenic region have been presented in the table).

Material	Temp. range (K)	S_r (%K ⁻¹)	Reference
[Tb _{0.914} Eu _{0.086}) ₂ (pda) ₃ (H ₂ O)]·2H ₂ O	10 – 325	5.96	9
Eu _{0.0069} Tb _{0.9931} -dmbdc	50 – 200	1.15	10
Eu _{0.2} Tb _{0.8} L	40 – 300	0.15	11
[Tb _{0.98} Eu _{0.02} (OA) _{0.5} (DSTP)]·3H ₂ O	75 – 275	6.53	12
Eu _{0.05} Tb _{0.09} Gd _{0.86} -DSB	20 – 65	2.37	13
Tb _{0.95} Eu _{0.05} HL	4 – 290	31.0	14
Eu: MoS ₂	60 – 360	1.49	15
(Me ₂ NH ₂) ₃ [Eu ₃ (FDC) ₄ (NO ₃) ₄]·4H ₂ O	12 – 320 K	2.70	16
P1	10 – 100	4.76	This work
P2	10 – 100	3.57	This work

References

- 1 H. Naruke, T, Yamase, *J. Lumin.*, **1991**, *50*, 55.
- 2 Agilent, CrysAlis Pro; Agilent Technologies UK Ltd, Yarnton, England: **2013**.
- 3 O. V. Dolomanov, L. J. Bourhis, R. J. Gildea, J. A. K. Howard, H. Puschmann, *J. Appl. Crystallogr.* **2009**, *42*, 339.
- 4 G. M. Sheldrick, *Acta Crystallogr. Sect. A*, **2008**, *64*, 112.
- 5 G. M. Sheldrick, *Acta Crystallogr. Sect. C*, **2015**, *71*, 3.
- 6 J. Garrevoet, B. Vekemans, S. Bauters, A. Demey, L. Vincze, *Anal. Chem.* **2015**, *87*, 6544.

- 7 B. Vekemans, K. Janssens, L. Vincze, F. Adams, P. Vanespen, *X-Ray Spectrom.* **1994**, *23*, 278.
- 8 T. Schoonjans, V. A. Solé, L. Vincze, M. Sanchez del Rio, K. Appel, C. Ferrero, A general Monte Carlo simulation of energy dispersive X-ray fluorescence spectrometers — Part 6. Quantification through iterative simulations. *Spectrochimica Acta Part B:Atomic Spectroscopy* **2013**, *82*, 36.
- 9 Z. P. Wang, D. Ananias, A. Carne-Sanchez, C. D. S. Brites, I. Imaz, D. MasPOCH, J. Rocha, L. D. Carlos, *Adv. Funct. Mater.* **2015**, *25*, 2824.
- 10 Y. J. Cui, H. Xu, Y. F. Yue, Z. Y. Guo, J. C. Yu, Z. X. Chen, J. K. Gao, Y. Yang, G. D. Qian, B. L. Chen, *J. Am. Chem. Soc.* **2012**, *134*, 3979.
- 11 S. N. Zhao, L. J. Li, X. Z. Song, M. Zhu, Z. M. Hao, X. Meng, L. L. Wu, J. Feng, S. Y. Song, C. Wang, H. J. Zhang, *Adv. Funct. Mater.* **2015**, *25*, 1463.
- 12 Y. Q. Wei, R. J. Sa, Q. H. Li, K. C. Wu, *Dalton Trans.* **2015**, *44*, 3067.
- 13 R. F. D'Vries, S. Alvarez-Garcia, N. Snejko, L. E. Bausa, E. Gutierrez-Puebla, A. de Andres, M. A. Monge, *J. Mater. Chem. C* **2013**, *1*, 6316.
- 14 X. Liu, S. Akerboom, M. de Jong, I. Mutikainen, S. Tanase, A. Meijerink, E. Bouwman, *Inorg. Chem.* **2015**, *54*, 11323.

15J. Liu, R. Van Deun, A. M. Kaczmarek, *J. Mater. Chem. C* **2016**, *4*, 9937.

16L. Li, Y. Zhu, X. Zhou, C. D. S. Brites, D. Ananias, Z. Lin, F. A. Almeida Paz, J. Rocha, W. Huang, L. D. Carlos, *Adv. Funct. Mater.* **2016**, DOI: 10.1002/adfm.201603179